WORLD CONFERENCE ON TIMBER ENGINEERING 2025
BRISBANE, AUSTRALIA

Advancing Timber for the Future Built Environment

EXPERIMENTAL STUDY OF STRUCTURAL PERFORMANCE OF TIMBER-CONCRETE COMPOSITES USING RECYCLED AGGREGATES

Daniel Kumah[1], Aamir Khokhar[2], Robert Hairstans[3]

ABSTRACT: This study analysed the structural performance of timber concrete composites (TCC) incorporating Incinerator Bottom Ash as recycled aggregates within the concrete constituent compared to normal aggregates concrete. Push-out test was conducted on twenty-four TCC specimens consisting of cross-laminated timber with either normal or recycled aggregate concrete layers, with screw connectors positioned at 90°, 45° or 30° in cross-inclined configuration to assess the load-slip behaviour, stiffness modulus and failure mechanisms. The results showed that recycled aggregate specimens achieved increased load-carrying capacity, improved slip between timber and concrete, and enhanced serviceability slip modulus comparable to normal aggregate concrete specimens. In addition, recycled aggregate specimens exhibited a similar failure mechanism to normal aggregate concrete specimens. The results demonstrate the potential of utilising recycled aggregates in TCC to promote sustainable construction.

KEYWORDS: Timber Concrete Composites, Push Out Test, Cross-Laminated Timber, Incinerator Bottom Ash Aggregates, Sustainable Construction

1 – INTRODUCTION

Timber-concrete composite (TCC) structures have become increasingly popular in modern construction because of their enhanced mechanical performance, sustainability and efficient utilisation of concrete's compressive strength and tensile capacity of timber [1]. In recent years, the integration of engineered wood products (EWP's) such as cross-laminated timber (CLT) has improved the load-carrying capacity and vibration performance of TCC's compared to traditional timber members alone [2], [3]. This enhanced structural performance has expanded the use of TCC as bridge decks and flooring systems in mid-story buildings globally [4], [5]. However, despite multiple benefits of TCC, there are significant concerns over environmental sustainability of concrete layer due to its reliance on natural aggregates and related embodied carbon. There is widespread interest in exploring sustainable alternatives to reduce the overall carbon footprint of TCC to promote eco-friendly construction and maximise structural performance [6], [7].

Rising greenhouse gas emissions in the construction sector is evident, emphasising the significance of incorporating sustainable concrete materials in composite building systems [8]. Some scholars have investigated the utilisation of lightweight concrete and high-strength concrete alternatives in TCC [9], [10]. However, large-scale production may be expensive despite their low self-weight and durability. Recycled aggregates from construction and demolition waste offer a cost-effective and renewable solution [11]. In addition, recycled aggregates sequester significant volumes of carbon depending on the degree of carbonation and cementitious content, which can potentially decrease net emissions in TCC applications [12].

Recycled aggregates such as Incinerator Bottom Ash (IBA) is unexplored in TCC; therefore, its utilisation presents an eco-friendly building material. IBA aggregates are obtained from waste-to-energy systems after combustion and processing of construction demolition and municipal solid waste [13]. They have a relatively

[1] Daniel Kumah, The School of Computing, Engineering and the Built Environment, Edinburgh Napier University, Edinburgh, United Kingdom, D.kumah@napier.ac.uk

[2] Aamir Khokhar, The School of Computing, Engineering and the Built Environment, Edinburgh Napier University, Edinburgh, United Kingdom, A.Khokhar@napier.ac.uk

[3] Robert Hairstans, The School of Computing, Engineering and the Built Environment, Edinburgh Napier University, Edinburgh, United Kingdom, R.hairstanshok@napier.ac.uk

https://doi.org/10.52202/080513-0244

lightweight and rough surface texture compared to virgin aggregates, which improves mechanical bonding with cement paste [14]. Gražulytė et al. established that recycled concrete produced from IBA aggregates exhibits similar strength and durability compared with C20/25 normal aggregates concrete [15]. Keulen et al. [16] also observed similar trends of robust mechanical performance using proportions of recycled aggregates in concrete, thus elevating its potential in sustainable TCC structures.

Notwithstanding the advantages of recycled aggregate in TCC, it exhibits considerable mechanical limitations due to unique characteristics such as high-water absorption rate, micro cracks and heterogeneous composition [17]. These properties affect concrete's compressive strength, ultimately influencing composite behaviour with shear connectors. Previous researchers have focused on the investigation of TCC using normal concrete layer with notches or dowel connectors and reported enhanced slip modulus and ductile failure mode with screws in inclined configuration [18], [19]. Therefore, this study seeks to examine the structural performance of TCC incorporating recycled aggregates in concrete layer with screw connectors at various penetration angles through a series of push-out tests in comparison with normal aggregate concrete layer TCC specimens. The load-slip behaviour, slip modulus and failure modes are assessed to evaluate the structural performance of sustainable TCC systems for further research and practical implementation.

2 – EXPERIMENTAL PROGRAM

2.1 TEST MATERIALS

Cross-laminated timber (CLT) is a widely used mass timber panel comprising of lumber arranged perpendicularly in adjacent layers and bonded with adhesives, providing bi-directional load resistance [20]. In this study, 90mm thick 3-ply CLT manufactured from *Sitka Spruce* softwood timber (120×30mm) of strength grade C24 was utilised in both longitudinal and transverse layers. The average density and moisture content of CLT samples were determined in accordance with BSEN 408 [21] and provided in Table 1.

The Building Research Establishment (BRE) mix design approach was used to proportion normal and recycled concrete mixes. Normal concrete comprised of quarried granite sand (0/5mm) and gravel with a maximum aggregate size of 20mm, having a saturated surface dry density (SDD) of 2640kg/m^3 and water absorption of 0.60%. Whereas IBA aggregates (0/20mm), with SSD of 2340kg/m^3 and water absorption capacity of 5.20% was used as a full replacement for coarse normal aggregates in recycled concrete. Glass fibre reinforcement was added to recycled concrete at a rate of 1.2kg/m^3 to control early-age cracking associated with recycled aggregates [22]. Ordinary Portland cement (OPC) of grade 52.5N was used as binder. The water-cement ratio (w/c) was maintained at 0.55 for all mixes to optimise strength and workability. Slump values were determined immediately after mixing as per BSEN 12350 [23] and concrete cubes were manufactured and tested for compressive strength at 28 days following BSEN 12390 [24] as shown in Figure 1. The mechanical properties of normal and recycled concrete are summarised in Table 1.

(a) (b)

Figure 1: *(a)Concrete cube compressive test at 28 days and (b) fresh concrete slump test*

Self-drilling screws with a nominal diameter of 6mm and an overall length of 100mm as shown in Figure 2, was used as shear connectors between timber and concrete. Screws are made of hardened carbon steel with corrosion-resistant coating for durable performance. The washer-head design enhances pull-out resistance in concrete, while the self-drilling tip eliminates the need for predrilling in timber [25]. Furthermore, the unthreaded shank in concrete reduces the initiation of thread-induced crack during shear transfer. The properties of screws as provided in manufacturer's technical document [26] is shown in Table 1.

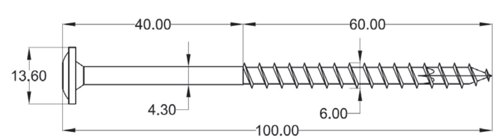

Figure 2: *Dimensions of self-drilling screws (mm)*

https://doi.org/10.52202/080513-0244

Table 1: Mechanical Properties of Materials

Material	Property	Value	Units
CLT	Density	459.97	kg/m^3
	Moisture Content	10.22	%
Recycled Concrete	Compressive Strength f_{cu}	29.09	MPa
	Density	2101.78	kg/m^3
	Slump	61.67	mm
Normal Concrete	Compressive Strength f_{cu}	36.29	MPa
	Density	2300.43	kg/m^3
	Slump	50.00	mm
Screws	Tensile Strength $f_{y,k}$	1000	N/mm^2
	Yield Moment $M_{y,Rk}$	9493.71	Nmm
	Modulus of Elasticity E_s	210000	MPa

2.2 SPECIMEN CONFIGURATION

A total of twenty-four TCC specimens were prepared for testing. The specimens were fabricated in six different groups, each comprising of four replicates of TCC specimens having either normal or recycled concrete layer with screw connectors positioned at 90°, 45° or 30° in cross-inclined configuration as summarised in Table 2. The specimens consisted of CLT panel (450×300×90mm), which were predrilled to facilitate precise screw insertion angle. The penetration depth of screws in CLT was selected as 10D (60mm) for optimum load transfer in timber as also employed by Du et al. [27]. Following edge distance criteria in Eurocode 5 [28], six screws were inserted on either side of CLT panel with a longitudinal spacing of 100mm and transverse interval of 150mm as shown in Figure 3. CLT panel was secured 50mm above the concrete layer within the formwork to allow vertical displacement during testing. Concrete was then cast on both sides of CLT. Each specimen was subsequently labelled to ensure specimen identification and efficient data collection, for instance, TCC-NC-S90, where TCC represents timber-concrete composites, NC signifies normal concrete, and S90 is the penetration angle of screws at 90°. A similar designation was used for recycled concrete specimens with RC replacing NC. Specimens were left to cure for at least 28 days under standard laboratory conditions as shown in Figure 4.

Table 2: Specimen configuration and main parameters

Specimen Configuration	Concrete Layer	Screw Angle/ Configuration	Insertion Depth [mm]	No. of Samples
TCC-NC-S90		90°		4
TCC-NC-S45	NC	45°	60	4
TCC-NC-S30		30°		4
TCC-RC-S90		90°		4
TCC-RC-S45	RC	45°	60	4
TCC-RC-S30		30°		4

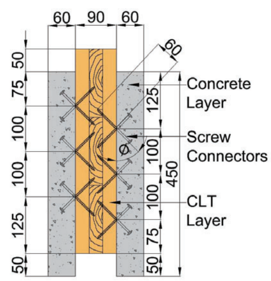

(a)

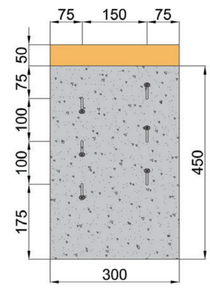

(b)

Figure 3: TCC specimen configuration and dimensions (mm)


(a)


(b)

Figure 4: (a) CLT positioned in formwork and (b) experimental TCC specimens

2.3 LOADING PROCEDURE

Push-out test of TCC specimens were carried out in accordance with BSEN 26891 [29]. The specimens were setup ensuring proper alignment with load cell and linear variable displacement transducers (LVDTs) as shown in Figure 5. Zwick Zoel Actuator, with 300kN load capacity was used to apply vertical force at a rate of 0.7mm/min until ultimate failure. The specimens were tested according to the loading profile in BSEN 26891 [29], to 40%F_{est}, then unloaded to 10%F_{est}, and thereafter loaded until failure as shown in Figure 6. The estimated failure load F_{est} was determined by testing one specimen in each group.

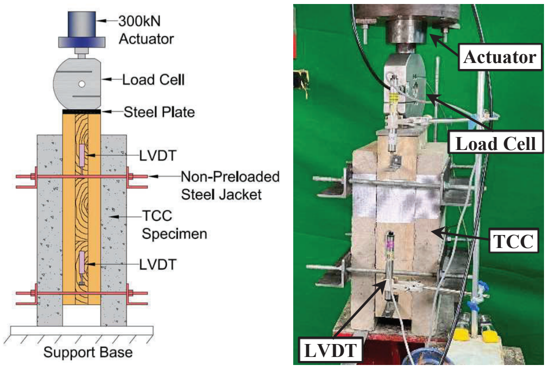

(a) (b)

Figure. 5: *Experimental setup of TCC specimens for push-out test*

The load-slip graph was plotted by taking the applied load recorded directly from the load cell and the average relative slip of four LVDTs with 25mm capacity attached to CLT. The main parameters determined include slip between timber and concrete (v), maximum applied force at failure (F_{max}) and slip modulus (k) according to BSEN26891 [29] using equation (1) to (5).

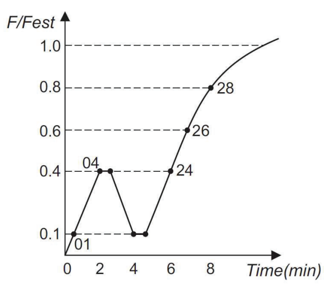

Figure 6: *Loading procedure according to BSEN 26891[29]*

$$k_i = \frac{0.4 \cdot F_{est}}{v_{0.4}} \tag{1}$$

$$k_{0.4} = \frac{0.4 \cdot F_{est}}{v_{i.mod}} \tag{2}$$

$$k_{0.6} = \frac{0.6 \cdot F_{est}}{v_{0.6} - v_{24} + v_{i.mod}} \tag{3}$$

$$k_{0.8} = \frac{0.8 \cdot F_{est}}{v_{0.8} - v_{24} + v_{i.mod}} \tag{4}$$

$$v_{i.mod} = \frac{4}{3} \cdot (v_{0.4} - v_{0.1}) \tag{5}$$

$v_{0.1}$, $v_{0.4}$, v_{24}, $v_{0.6}$, $v_{0.8}$ are slips recorded during push out test corresponding to $0.1F_{est}$, $0.4F_{est}$, $0.4F_{est}$ (during second loading cycle), $0.6F_{max}$ and $0.8F_{max}$ respectively. $v_{i.mod}$ is modified initial slip whereas k_i represents initial slip, $k_{0.4}$ is serviceability slip modulus (k_{ser}), $k_{0.6}$ is ultimate slip modulus (k_{ult}), and $k_{0.8}$ is the slip modulus at collapse in kN/mm.

3 – RESULTS AND DISCUSSION

The push-out test revealed different load-slip responses of TCC specimens with either normal or recycled aggregates and screw penetration angle as shown in Figure 7. All Specimens exhibited an initial linear-elastic behaviour followed by concrete cracking noise with loss of stiffness and gradual non-linear increase in applied load until maximum force was reached. Parameters such as slip (relative displacement between timber and concrete layer), slip modulus (stiffness of screw connection in TCC), ultimate load (the maximum load before collapse) and failure mode of each specimen were analysed and summarised in Table 3.

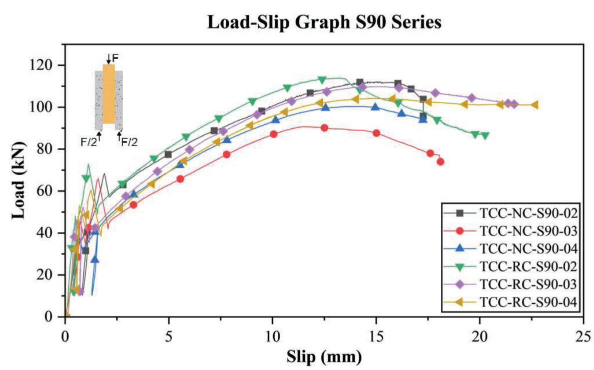

Figure 7a: *Load-slip graph for normal concrete (NC) and recycled concrete (RC) specimens with 90° screw inclination*

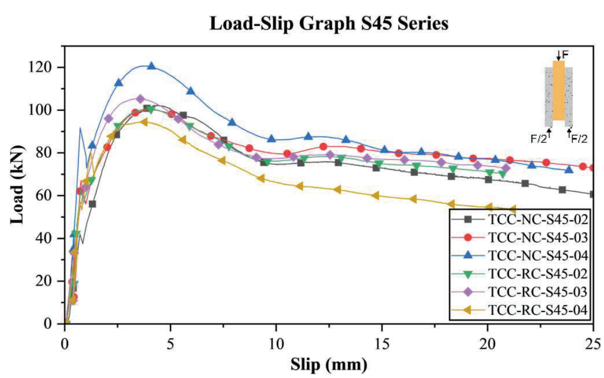

Figure 7b: *Load-slip graph for normal concrete (NC) and recycled concrete (RC) specimens with 45° screw inclination*

https://doi.org/10.52202/080513-0244

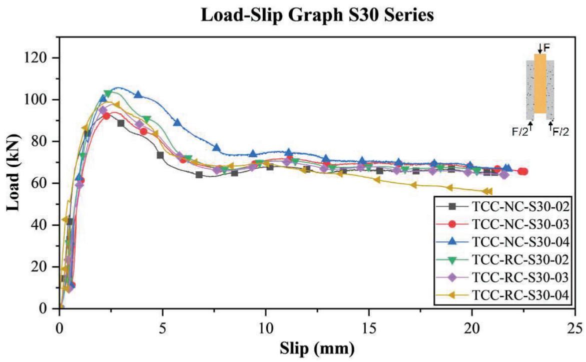

Figure 7c: *Load-slip graph for normal concrete(NC) and recycled concrete (RC) specimens with 30° screw inclination*

3.1 INFLUENCE OF CONCRETE LAYER

The type of concrete layer significantly influenced the structural performance and composite behaviour of TCC specimens. NC specimens with inclined screw configuration consistently exhibited higher load-carrying capacity and improved stiffness than RC specimens. For instance, the average maximum load for RC specimens with 45° screws was 9% lower than NC specimens. Similarly, 30° RC specimens showed a 5% decrease in peak load relative to NC specimens. However, 90° RC specimens achieved an average ultimate force of 8% higher than identical NC specimens despite low compressive strength. Improved ductility of RC and significant interlayer frictional resistance during rope effect contributed to greater load capacity in vertical screw specimens.

Interlayer slip between concrete and timber varied by concrete layer type with inclined screw RC specimens exhibiting 4-10% lower slips than similar NC specimens. The average slip recorded for 45° NC specimens was 4.08mm compared to 3.68mm by RC specimens. Likewise, 30° NC specimens achieved a mean slip of 2.63mm compared with 2.51mm by RC specimen. On the other hand, 90° RC specimens exhibited 6% increase in average slip compared to 13.48mm by NC specimens. Thus, voids and cracks within the microstructure of RC redistributed high shear stresses in vertical screws, resulting in small deformations and increased slip. RC specimens consistently exhibited a low percentage coefficient of variation (CoV) of 7%, whereas NC specimens had 7-14%, indicating improved consistency in slip values for RC specimens.

Serviceability slip modulus of RC specimens with inclined screws was slightly lower than similar NC specimens. 45° NC specimens attained a slip modulus of 112.33kN/mm, while matching RC specimens showed 18% decrease. Likewise, 30° RC specimens experienced 5% loss in slip modulus compared to NC specimens. However, in the case of 90° RC specimens, the mean serviceability slip modulus was 110% greater than NC specimens.

The findings reveal that, although NC specimens provided superior load-carrying capacity and stiffness with inclined screws, RC specimens exhibited comparable structural performance despite relatively low compressive strength, signifying exceptional screw engagement and gradual load transfer with inclined screws. However, vertical screw RC specimens exhibited comparatively higher slip and increased slip modulus than NC counterparts due to improved ductility and significant interlayer frictional resistance.

3.2 INFLUENCE OF SCREW INCLINATION

TCC specimens with cross-inclined screws outperformed vertical screws in slip values and stiffness modulus. A similar screw behaviour was also noted by Mirdad et al. [25]. 90° NC specimens achieved a mean maximum slip of 13.52mm, which decreased by 70% and 81% in 45° and 30° specimens respectively. However, 45° and 30° RC specimens exhibited slightly lower slips of 10% and 4% than similar NA specimens while achieving increased slip of 6% for 90° specimens. This pattern aligns with previous research findings highlighting the effective load distribution and reduced interlayer slip of inclined screws in TCC [30]. Moreover, the low CoV of 7-10% of inclined screw specimens indicates enhanced predictability of interlayer slip.

Inclined screw specimens maintained an upward trend in slip modulus compared to vertical screws. For NC specimens, the serviceability slip modulus increased by 166% for 45° specimens and achieved 115% increase for 30° specimens relative to 90° specimens, which attained a serviceability slip modulus of 42.21kN/mm. In the same way, slip modulus in 90° RC specimens was 88.55kN/mm which improved by 5% at 45° and experienced a 3% reduction at 30° screw inclination. Although inclined screw RC specimens exhibited lower stiffness values compared with NC specimens, the overall trend of increased slip modulus with inclined screws was consistent.

These results highlight the effectiveness of angled screws in enhancing slip and stiffness modulus of RC specimens. In addition, mechanical engagement of inclined screw marginally mitigated the effects of low compressive strength of RC on composite behaviour.

3.3 FAILURE MODES

Three primary failure modes were identified during the push-out test: concrete cracking, screw yielding and crushing of timber fibres around screw. The failure mechanism was mainly influenced by screw inclination angle and type of concrete layer. 90° normal and recycled concrete specimens predominantly experienced concrete cracking around screws resulting in the splitting of concrete section as shown in Figure 8a and Figure 8b. This failure mode reflects high shear concentrations often localised around vertical screws [9]. However, the severity of cracking was minimal with decreasing screw inclination due to the balance of shear and axial force resulting in reduced stress concentrations as shown in Figure 8c and Figure 8d. Concrete cracking occurred less frequently across inclined screw RC specimens. Moreover, glass fibres in RC contributed to controlling crack propagation.

Inclined screw specimens exhibited yielding before any significant damage to concrete, while vertical screw specimens showed instances of severe concrete cracking around connectors. Compression screws exhibited double plastic hinges and failure in surrounding concrete, while tensile screws showed single plastic hinge and withdrawal in timber as shown in Figure 7. This failure mechanism of screws was also observed by other authors [31]. 90° screw specimens showed similar plastic hinges at ultimate load. The degree of yielding in 90° and 45° specimens was more pronounced than in 30° specimens, as shown in Figure 8e-8g. Plastic deformations across NC and RC specimens were synonymous with the European yield model's failure mode (e and f) in Eurocode 5 [28].

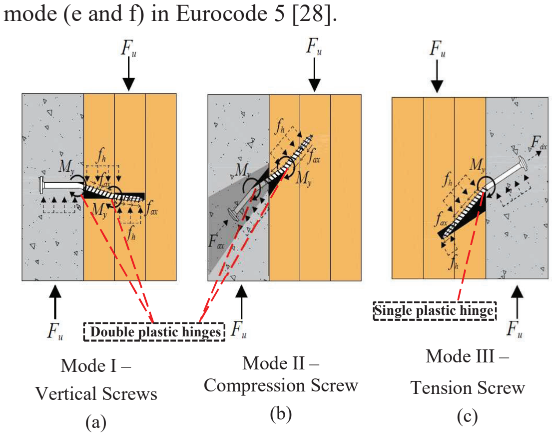

Figure 7: *Failure mechanism of screws in timber and concrete layer for 90° screw orientation (a) and inclined screws in compression (b) and tension (c)*

Timber embedment was characterised by localised deformation of timber fibres around screws as shown in Figure 8h. Embedment depth was found to be higher with inclined screw specimens signifying efficient engagement of timber fibres and effective load transfer, particularly 45° specimens. The ductility of RC also enhanced stress redistribution around screws, resulting in less pronounced embedment failure in timber. Figure 8 shows the failure modes of TCC specimens.

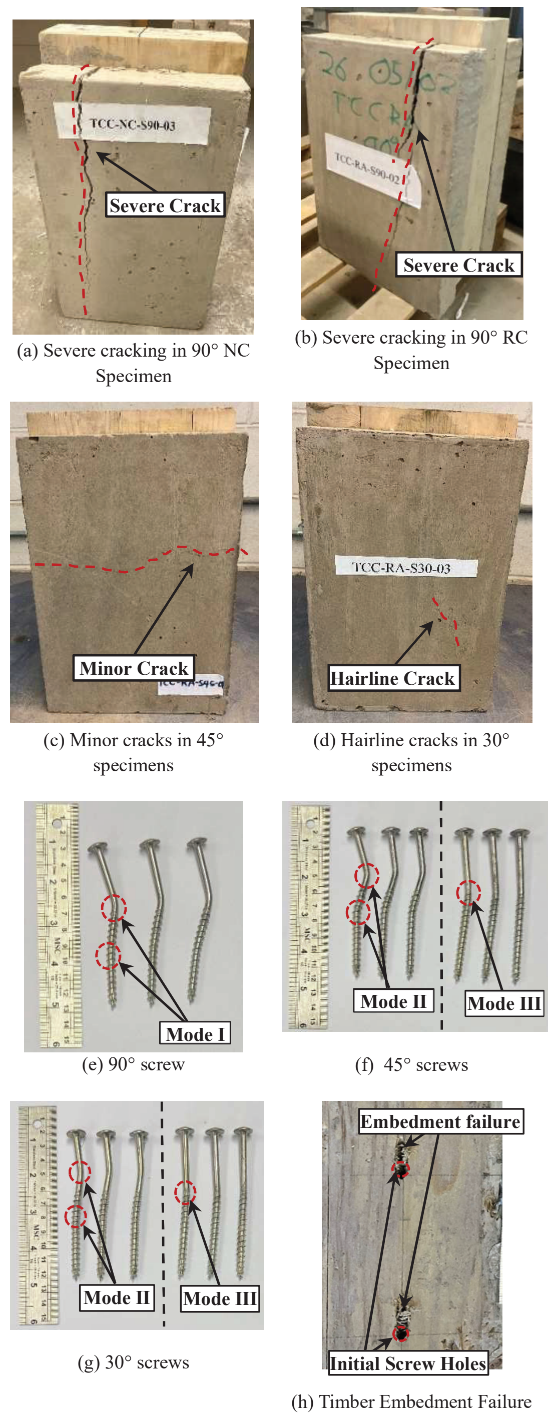

(a) Severe cracking in 90° NC Specimen
(b) Severe cracking in 90° RC Specimen
(c) Minor cracks in 45° specimens
(d) Hairline cracks in 30° specimens
(e) 90° screw
(f) 45° screws
(g) 30° screws
(h) Timber Embedment Failure

Figure 8: *Failure Mode of concrete, timber and screws of TCC specimens*

https://doi.org/10.52202/080513-0244

Table 3: Experimental results from push out test

Specimen ID	F_{est} / F_{max} [kN]	δ_{max} [mm]	$k_{i\,0.4}$ [kN/mm]	k_{ser} [kN/mm]	k_{ult} [kN/mm]	$k_{0.8}$ [kN/mm]	Failure Mode
*TCC-NC-90°-01	103.65	11.69					(a) + (e) + (h)
TCC-NC-90°-02	111.98	15.00	39.44	36.42	18.75	11.15	
TCC-NC-90°-03	90.79	11.48	62.48	65.92	17.94	12.09	
TCC-NC-90°-04	100.37	14.07	27.56	24.27	17.29	11.87	
Average	101.05	13.52	43.16	42.21	17.99	11.70	
	(10.50)	(13.48)	(41.14)	(50.74)	(10.69)	(4.24)	
*TCC-NC-45°-01	72.02	3.75					(c) + (f) + (h)
*TCC-NC-45°-02	102.38	4.44					
TCC-NC-45°-03	100.03	4.27	73.96	98.36	56.48	43.68	
TCC-NC-45°-04	120.68	3.89	96.49	126.30	59.83	46.80	
Average	110.35	4.08	85.22	112.33	58.16	45.24	
	(13.23)	(6.59)	(18.70)	(17.59)	(4.08)	(4.88)	
*TCC-NC-30°-01	109.29	2.96					(d) + (g) + (h)
TCC-NC-30°-02	92.78	2.35	96.95	121.12	108.25	92.06	
TCC-NC-30°-03	93.99	2.69	57.30	69.76	67.91	64.15	
TCC-NC-30°-04	105.83	2.85	64.57	81.74	68.85	58.64	
Average	97.53	2.63	72.94	90.87	81.67	71.62	
	(7.39)	(9.73)	(28.94)	(29.57)	(28.19)	(25.02)	
*TCC-RC-90°-01	116.00	15.00					(b) + (e) + (h)
TCC-RC-90°-02	113.89	13.22	98.03	107.44	21.07	13.87	
TCC-RC-90°-03	109.78	15.00	64.38	71.51	17.48	12.35	
TCC-RC-90°-04	104.18	14.93	75.96	86.69	17.12	12.67	
Average	109.28	14.39	79.46	88.55	18.55	12.96	
	(4.46)	(7.00)	(21.52)	(20.37)	(11.76)	(6.16)	
*TCC-RC-45°-01	105.86	3.90					(c) + (f) + (h)
TCC-RC-45°-02	100.65	3.93	78.56	110.29	62.92	46.60	
TCC-RC-45°-03	105.30	3.39	73.62	76.59	66.28	55.17	
TCC-RC-45°-04	94.71	3.71	75.36	91.14	74.04	53.77	
Average	100.22	3.68	75.85	92.67	67.75	51.85	
	(5.30)	(7.30)	(3.30)	(18.24)	(8.42)	(8.87)	
*TCC-RC-30°-01	92.644	2.27					(d) + (g) + (h)
TCC-RC-30°-02	103.50	2.55	66.22	91.04	60.49	55.61	
TCC-RC-30°-03	97.71	2.67	61.27	70.98	57.65	54.42	
TCC-RC-30°-04	99.13	2.33	81.90	95.83	87.96	72.13	
Average	100.11	2.51	69.80	85.95	68.70	60.72	
	(3.02)	(6.75)	(15.43)	(15.34)	(24.37)	(16.30)	

* Estimated failure load specimens
(x) represents the coefficient of variation CoV[%]

4–CONCLUSION

This study investigated the structural performance of TCC using recycled concrete in comparison to normal concrete layer. The influence of screw penetration angle on load-carrying capacity, slip behaviour, slip modulus and failure mechanism was also examined.

The results demonstrate that while minor reductions in slip modulus and a slight increase in slip were observed in recycled concrete specimens, overall structural behaviour and load-carrying capacity were significantly comparable to normal concrete TCC specimens. Recycled concrete specimens exhibited identical failure characteristics to normal concrete specimens. The screw penetration angle influenced the severity of concrete fracture, degree of screw plastic hinge deformation and depth embedment failure in timber. Inclined screw specimens experienced minor concrete cracking and screw yielding than vertical screw specimens signifying efficient load transfer between timber and concrete with angled screws. Moreover, the ductility of recycled concrete also enhanced stress distribution around screws, resulting in less pronounced local crushing of timber fibres around screws and concrete cracking. Recycled TCC specimens exhibited a 10% decrease in self-weight due to the lightweight of recycled aggregate concrete compared to normal aggregate concrete, making them suitable for long-span applications. These results highlight the potential of incorporating recycled concrete in TCC, making it a promising solution for sustainable and lightweight TCC construction.

Additional investigation using finite element modelling approach and long-term durability performance of timber-recycled concrete composites could be explored to further analyse its behaviour to promote widespread adoption.

ACKNOWLEDGEMENTS

Special thanks to Built Environment-Smarter Transformation (BE-ST) for manufacturing and providing cross-laminated timber samples. Our sincere appreciation to LEAVENSEAT, a commercial recycling and waste management industry, for supplying Incinerator Bottom Ash for use as recycled aggregates in this research.

REFERENCES

[1] A. Dias, J. Skinner, K. Crews, and T. Tannert, ‘Timber-concrete-composites increasing the use of timber in construction’, European Journal of Wood and Wood Products, vol. 74, no. 3, pp. 443–451, 2016, doi: 10.1007/s00107-015-0975-0.

[2] M. Van Thai, S. M. Elachachi, S. Ménard, and P. Galimard, ‘Vibrational behavior of cross-laminated timber-concrete composite beams using notched connectors’, Eng Struct, vol. 249, p. 113309, Dec. 2021, doi: 10.1016/J.ENGSTRUCT.2021.113309.

[3] A. Ogrin and T. Hozjan, ‘Fire resistance of timber-concrete composite slabs’, Mater Struct, vol. 53, no. 4, p. 106, 2020, doi: 10.1617/s11527-020-01540-6.

[4] Z. Lyu, C. Málaga-Chuquitaype, and A. M. Ruiz-Teran, ‘Design of timber-concrete composite (TCC) bridges with under-deck stay cables’, Eng Struct, vol. 189, pp. 589–604, Jun. 2019, doi: 10.1016/J.ENGSTRUCT.2019.03.059.

[5] J. Estévez-Cimadevila, E. Martín-Gutiérrez, F. Suárez-Riestra, D. Otero-Chans, and J. A. Vázquez-Rodríguez, ‘Timber-concrete composite structural flooring system’, Journal of Building Engineering, vol. 49, p. 104078, May 2022, doi: 10.1016/J.JOBE.2022.104078.

[6] M. A. H. Mirdad, H. Daneshvar, T. Joyce, and Y. H. Chui, ‘Sustainability Design Considerations for Timber-Concrete Composite Floor Systems’, Advances in Civil Engineering, vol. 2021, no. 1, p. 6688076, 2021, doi: https://doi.org/10.1155/2021/6688076.

[7] L. Corti and G. Muciaccia, ‘Stiffness Warming Potential: An Innovative Parameter for Structural and Environmental Assessment of Timber–Concrete Composite Members’, Sustainability, vol. 15, no. 20, 2023, doi: 10.3390/su152014857.

[8] R. Modi and A. Bhogayata, ‘Utilization of recycled concrete residues as secondary materials in the development of sustainable concrete composite’, Mater Today Proc, Apr. 2023, doi: 10.1016/J.MATPR.2023.03.664.

[9] E. Appavuravther, B. Vandoren, and J. Henriques, ‘Behaviour of screw connections in timber-concrete composites using low strength lightweight concrete’, Constr Build Mater, vol. 286, p. 122973, Jun. 2021, doi: 10.1016/J.CONBUILDMAT.2021.122973.

[10] S. Lamothe, L. Sorelli, P. Blanchet, and P. Galimard, ‘Lightweight and slender timber-concrete composite floors made of CLT-HPC and CLT-UHPC with ductile notch connectors’, Eng Struct, vol. 243, p. 112409, Sep. 2021, doi: 10.1016/J.ENGSTRUCT.2021.112409.

[11] S. Shahidan, M. A. M. Azmi, K. Kupusamy, S. S. M. Zuki, and N. Ali, ‘Utilizing Construction and Demolition (C&D) Waste as Recycled Aggregates (RA) in Concrete’, Procedia Eng, vol. 174, pp. 1028–1035, Jan. 2017, doi: 10.1016/J.PROENG.2017.01.255.

[12] A. Leemann, B. Münch, and M. Wyrzykowski, ‘CO2 absorption of recycled concrete aggregates in natural conditions’, Mater Today Commun, vol. 36, p. 106569, Aug. 2023, doi: 10.1016/J.MTCOMM.2023.106569.

[13] Y. Cheng et al., ‘Physical and mechanical study of municipal solid waste incineration (MSWI) bottom ash with different particle size distribution’, Constr Build Mater, vol. 416, p. 135137, Feb. 2024, doi: 10.1016/J.CONBUILDMAT.2024.135137.

[14] Z. Li et al., ‘Research on the durability and Sustainability of an artificial lightweight aggregate concrete made from municipal solid waste incinerator bottom ash (MSWIBA)’, Constr Build Mater, vol. 365, p. 129993, Feb. 2023, doi: 10.1016/J.CONBUILDMAT.2022.129993.

https://doi.org/10.52202/080513-0244

[15] J. Gražulytė, A. Vaitkus, O. Šernas, and L. Žalimienė, ‘The impact of MSWI bottom ash as aggregate on concrete mechanical performance’, International Journal of Pavement Engineering, vol. 23, no. 9, pp. 2903–2911, Jul. 2022, doi: 10.1080/10298436.2021.1873333.

[16] A. Keulen, A. Van Zomeren, P. Harpe, W. Aarnink, H. A. E. Simons, and H. J. H. Brouwers, ‘High performance of treated and washed MSWI bottom ash granulates as natural aggregate replacement within earth-moist concrete’, Waste Management, vol. 49, pp. 83–95, Mar. 2016, doi: 10.1016/J.WASMAN.2016.01.010.

[17] G. Bai, C. Zhu, C. Liu, and B. Liu, ‘An evaluation of the recycled aggregate characteristics and the recycled aggregate concrete mechanical properties’, Constr Build Mater, vol. 240, p. 117978, Apr. 2020, doi: 10.1016/J.CONBUILDMAT.2019.117978.

[18] S. Di Nino, A. Gregori, and M. Fragiacomo, ‘Experimental and numerical investigations on timber-concrete connections with inclined screws’, Eng Struct, vol. 209, p. 109993, Apr. 2020, doi: 10.1016/J.ENGSTRUCT.2019.109993.

[19] M. A. H. Mirdad and Y. H. Chui, ‘Stiffness prediction of Mass Timber Panel-Concrete (MTPC) composite connection with inclined screws and a gap’, Eng Struct, vol. 207, p. 110215, Mar. 2020, doi: 10.1016/J.ENGSTRUCT.2020.110215.

[20] H. Li, B. J. Wang, P. Wei, and L. Wang, ‘Cross-laminated Timber (CLT) in China: A State-of-the-Art’, Journal of Bioresources and Bioproducts, vol. 4, no. 1, pp. 22–31, Feb. 2019, doi: 10.21967/JBB.V4I1.190.

[21] British Standard Institution, ‘BSEN408:2010+A1:2012- Timber Structures - Structural timber and glued laminated timber-Determination of some physical and mechanical properties’, London, UK, 2011.

[22] Y. Chen, Q. He, X. Liang, R. Jiang, and H. Li, ‘Experimental investigation on mechanical properties of glass fiber reinforced recycled aggregate concrete under uniaxial cyclic compression’, Cleaner Materials, vol. 6, p. 100164, Dec. 2022, doi: 10.1016/J.CLEMA.2022.100164.

[23] British Standard Institution, ‘BS EN 12350-2:2019. Testing fresh concrete. Slump test’, London, UK, 2019.

[24] British Standard Institution, ‘BSEN 12390-3:2019 - Testing hardened concrete-Part 3: Compressive strength of test specimens’, London, UK, 2019.

[25] M. A. H. Mirdad and C. YingHei, ‘Load-slip performance of Mass Timber Panel-Concrete (MTPC) composite connection with Self-Tapping Screws and insulation layer.’, Constr Build Mater, vol. 213, pp. 696–708, 2019.

[26] European Organization for Technical Approvals (EOTA), ‘European Technical Assessment ETA-12/0114: SPAX self-tapping screws. Screws for use in timber constructions’, Denmark, 2024.

[27] H. Du, X. Hu, Z. Xie, and H. Wang, ‘Study on shear behavior of inclined cross lag screws for glulam-concrete composite beams’, Constr Build Mater, vol. 224, pp. 132–143, Nov. 2019, doi: 10.1016/J.CONBUILDMAT.2019.07.035.

[28] British Standard Institution, ‘BSEN 1995-1-1:2004+A2:2014 Eurocode 5. Design of timber structures. General. Common rules and rules for buildings’, London, UK, 2004.

[29] British Standard Institute, ‘BS EN 26891:1991-Timber structures. Joints made with mechanical fasteners. General principles for the determination of strength and deformation characteristics’, London, UK, 1991.

[30] G. Y. Jeong, V. S. Pham, and D. K. Tran, ‘Development of predicting equations for slip modulus and shear capacity of CLT–concrete composite with screw connections’, Journal of Building Engineering, vol. 71, p. 106468, Jul. 2023, doi: 10.1016/J.JOBE.2023.106468.

[31] H. Du, X. Hu, G. Han, and D. Shi, ‘Experimental and analytical investigation on flexural behaviour of glulam-concrete composite beams with interlayer’, Journal of Building Engineering, vol. 38, p. 102193, Jun. 2021, doi: 10.1016/J.JOBE.2021.102193.